Received: 2 March 2017 | Revised: 6 June 2017 | Accepted: 5 July 2017

DOI: 10.1002/pip.2923

WILEY PROGRESS IN PHOTOVOLTAICS

RESEARCH ARTICLE

Proton irradiation of CdTe thin film photovoltaics deposited on cerium-doped space glass

Dan A. Lamb[1] | Craig I. Underwood[2] | Vincent Barrioz[3] | Russell Gwilliam[4] | James Hall[5] | Mark A. Baker[2] | Stuart J.C. Irvine[1]

[1] College of Engineering, Swansea University, Centre for Solar Energy Research, UK

[2] Department of Electronic Engineering, University of Surrey, UK

[3] Department of Mathematics, Physics, and Electrical Engineering, Northumbria University, UK

[4] Advanced Technology Institute, University of Surrey, UK

[5] Qioptiq Ltd, Qioptiq Space Technology, UK

Correspondence
Dan A. Lamb, Centre for Solar Energy Research, College of Engineering, Swansea University, SA1 8EN UK .
Email: d.a.lamb@swansea.ac.uk

Funding information
Engineering and Physical Science Research Council, Grant/Award Number: EP/K019597/2 and EP/K019597/1

Abstract

Space photovoltaics is dominated by multi-junction (III-V) technology. However, emerging applications will require solar arrays with high specific power (kW/kg), flexibility in stowage and deployment, and a significantly lower cost than the current III-V technology offers. This research demonstrates direct deposition of thin film CdTe onto the radiation-hard cover glass that is normally laminated to any solar cell deployed in space. Four CdTe samples, with 9 defined contact device areas of 0.25 cm^2, were irradiated with protons of 0.5-MeV energy and varying fluences. At the lowest fluence, 1×10^{12} cm^{-2}, the relative efficiency of the solar cells was 95%. Increasing the proton fluence to 1×10^{13} cm^{-2} and then 1×10^{14} cm^{-2} decreased the solar cell efficiency to 82% and 4%, respectively. At the fluence of 1×10^{13} cm^{-2}, carrier concentration was reduced by an order of magnitude. Solar Cell Capacitance Simulator (SCAPS) modelling obtained a good fit from a reduction in shallow acceptor concentration with no change in the deep trap defect concentration. The more highly irradiated devices resulted in a buried junction characteristic of the external quantum efficiency, indicating further deterioration of the acceptor doping. This is explained by compensation from interstitial H^+ formed by the proton absorption. An anneal of the 1×10^{14} cm^{-2} fluence devices gave an efficiency increase from 4% to 73% of the pre-irradiated levels, indicating that the compensation was reversible. CdTe with its rapid recovery through annealing demonstrates a radiation hardness to protons that is far superior to conventional multi-junction III-V solar cells.

KEYWORDS

cadmium telluride, photovoltaic cells, proton radiation, space technology, thin film solar cells

1 | INTRODUCTION

The Centre for Solar Energy Research (CSER), Swansea University in collaboration with the University of Surrey has developed a thin film cadmium telluride (CdTe) solar cell technology for use in Space.[1-3] Working with industrial partners Qioptiq Space Technology (QST) and Surrey Satellite Technology Ltd, this solar cell technology is designed to meet the emerging demands of new space applications.

There are currently over 2000 operational satellites in Earth's orbit, with power requirements from a few Watts to 10's of kW in the most part satisfied by solar photovoltaics (PV). The power-to-weight ratio, the operational lifetime, and the cost/Watt of PV are critical parameters for the success of extra-terrestrial missions. Initially, for space application, silicon PV was employed; starting with the Vanguard 1 mission in 1958, but since the late 1990s, space missions have favoured multi-junction (III-V) PV with its high-power density (kW/m^2) and beginning-of-life (BOL) efficiency of around 30%. However, there are emerging applications which will require solar arrays with high specific power (kW/kg), flexibility in stowage and deployment, and a significantly lower cost than is currently available.[4] New space PV technologies need to be developed to meet the needs of future advances in space exploration and energy harvesting. Some

of these predicted advances include large constellations in space or fixed lunar/Martian bases, solar electric propulsion (SEP),[5] and Space-based Solar Power (SBSP).[6] The latter is a method of collecting solar power in space for use on Earth exploiting the exposure to higher (than terrestrial) intensity sunlight, with near 24 hour-a-day operation and no climatic interference.

Solar cells deployed in space are subject to high intensity radiation which is conventionally mitigated by covering with a cerium doped cover glass. The cover glass provides a pathway for the absorption of high intensity radiation that would darken any conventional glass.[7] The thickness of this glass determines the intensity of proton and electrons that are absorbed and is chosen depending upon the mission orbit and hence radiation environment that the solar cells are to be deployed in.

The innovative step of this research is to directly deposit thin film CdTe onto the cover glass thus saving on the weight and additional cost of having to use a substrate material:

- The cover glass is flexible allowing it to be "rolled up" before and after the solar cell is applied to it.
- This flexibility enables a cost-reducing roll-to-roll manufacturing process.
- A flexible solar cell technology for space will enable reduction of stowage volume and new pathways for subsequent deployment.

A 100 micron, chemically toughened and cerium-doped cover glass has been supplied by Qioptiq Space Technology for this research.[8] However, this and previous studies indicate that the polycrystalline CdTe material could be more radiation hard than other materials. Bätzner et al stated that, for CdTe, "onset of cell degradation typically occurs at particle fluences, which are 2 orders of magnitude higher than that conventionally experienced by monocrystalline space solar cells of Si or III–V compounds".[9] This high level of radiation hardness, for CdTe, will potentially allow for a far thinner and therefore lighter cover glass than is used for conventional III-V devices.

Previous research into the proton degradation of CdTe solar cells has been influenced by generation of colour centres within the glass superstrates typically used.[9-11] G. Yang et al deposited CdTe onto Corning™ ultra-thin 100-micron glass and subjected samples to 15-MeV energy of protons through the glass side.[11] Using fluences of between 1×10^{12} cm^{-2} and 1×10^{15} cm^{-2}, their results were affected by a reduction in short-circuit current through a darkening of the non-radiation hard glass superstrate. This effective darkening of the glass reduces transmission of photons through to the PV material. It is a fast process and rapidly reduces the photo-current of the PV devices. This paper is the first to report the proton radiation hardness of CdTe deposited onto cerium-doped cover glass. Unlike any previous studies, the proton irradiation will not appreciably darken the glass superstrate, and hence the superstrate will not contribute to any additional loss of short circuit current within the device.

For these experiments, a proton energy of 0.5 MeV and irradiation directly applied to the CdTe face has been chosen to ensure penetration through the active layers into the glass substrate, and yet to maximise any potential proton damage within the polycrystalline semiconductor layer. Four fluences have been used to simulate different orbital environments and durations of missions.

2 | EXPERIMENTAL

2.1 | Device structure

The solar cell materials were deposited using metal organic chemical vapour deposition (MOCVD). The cells follow a superstrate configuration, see Figure 1, where 800 nm of Al-doped ZnO (AZO) and 100 nm of undoped ZnO buffer layer were deposited directly onto the chemically toughened 100-μm cerium-doped cover glass using MOCVD. The AZO/ZnO layers are followed by a 25-nm CdS seed layer and 125 nm CdZnS window layer before deposition of 3.25 μm of As-doped CdTe absorber layer. The As-doping of the CdTe layer is graded to produce an As concentration of 3×10^{18} cm^{-3} in the first 3.0 μm and 1×10^{19} cm^{-3} in the final 250 nm, reducing the back surface contact resistance. Solar cell devices were formed by addition of evaporated gold back contacts, the area of which defined the area of each cell.

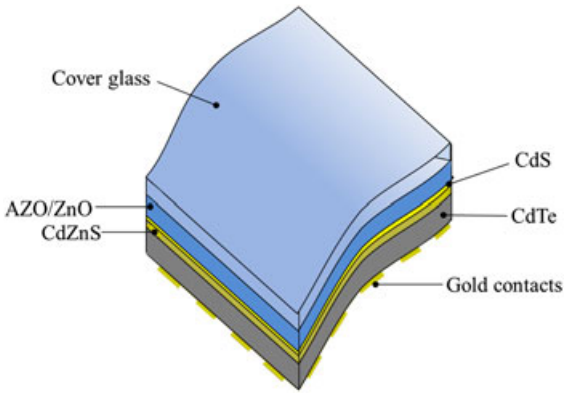

FIGURE 1 CdTe solar cell on ultra-thin cerium-doped cover glass structure [Colour figure can be viewed at wileyonlinelibrary.com]

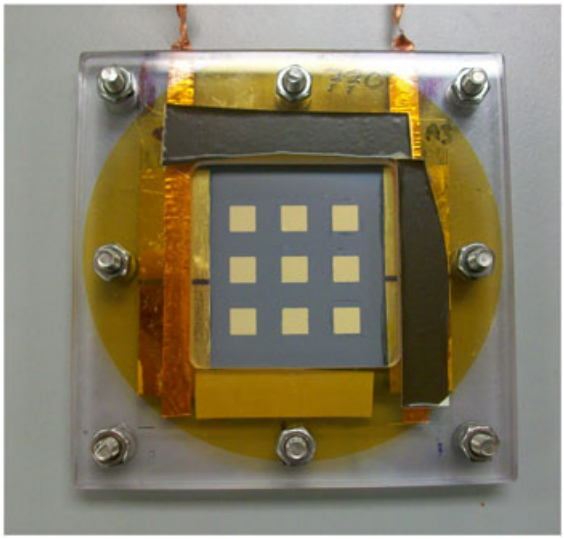

FIGURE 2 Sample 4 in Perspex sample holder after irradiation with highest proton fluence 1×10^{15} cm^{-2} [Colour figure can be viewed at wileyonlinelibrary.com]

For the work presented in this paper, 9 × 0.25 cm^2 cells were prepared on each of the 5 deposited samples. The 9 cells share a common front contact (the AZO/ZnO) which is revealed by removing the CdTe/CdZnS on 2 opposite sides of the sample followed by gold evaporation onto the exposed AZO/ZnO. Electrical probing is then made possible by contact to both the revealed AZO/ZnO strips with copper tape clamped in place and a gold probe contact to each of the 0.25-cm^2 gold square back contacts (see Figure 2).

In this configuration, it was possible to measure the electrical continuity across the TCO providing a useful metric to be collected at different stages of the irradiation. This bus-bar-to-bus-bar (B2B) value was found to be between 4 and 9 Ω for the 5 samples and did not vary significantly before or after the proton irradiation.

2.2 | Proton irradiation

Proton irradiation of the cells was performed at normal incidence to the CdTe/gold back contact face. The proton irradiation was carried out at the Surrey Ion Beam Centre using the 2 MV van de Graaff ion implanter, which is an Engineering and Physical Sciences Research Council (EPSRC) Central Facility. The implanter is capable of implanting ions at energies between 2 keV and 4 MeV, into sample sizes ranging from ~mm^2 to 40 cm^2. The samples may be held at constant temperatures ranging from ~1270 to ~77 K. Beam currents up to 10 mA were available, so that, even at the high particle fluences, the irradiations could be completed within a day.

To plan the tests, several simulations were carried out using the Stopping and Range of Ions in Matter (SRIM) 2008.04 software.[12] The cell was modelled as a composite consisting of the following layers:

- 3250-nm CdTe (ICRU-346; 5.85 $g.cm^{-3}$)
- 150-nm CdZnS (1:1:1 ratio; 4.46 $g.cm^{-3}$)
- 100-nm ZnO (1:1 ratio; 5.61 $g.cm^{-3}$)
- 800-nm AZO (2:50:50 ratio; 5.61 $g.cm^{-3}$)
- 100-μm boro-silicate glass (2.60 $g.cm^{-3}$)

Various energies of protons at normal incidence on the CdTe face were simulated. The total thickness of the semiconductor layers was 4.3 microns. The SRIM simulations showed that, given the material densities, 0.5-MeV protons would pass through all the active layers and also cause the maximum damage in terms of ionization energy absorbed (~17 eV/Å) and displacement damage (21 displacements per proton, 939 eV per recoil), see Figure 3. At energies, higher than 0.55 MeV, the SRIM simulations showed that protons pass through the structure with relatively little interaction and that the ionized energy is significantly lower.

Four proton fluences were selected to examine the CdTe solar cell performance under increasing dose levels (1 × 10^{12} cm^{-2}, 1 × 10^{13} cm^{-2}, 1 × 10^{14} cm^{-2}, and 1 × 10^{15} cm^{-2}). The particle spectrum in Earth orbit is complex, comprising the trapped electrons and protons of the van Allen belts, as well as protons and heavy ion cosmic rays—both from Galactic and solar origin. Because of this, for predictions of solar cell performance in orbit, the environments are reduced to "equivalent fluxes" of 1-MeV electrons and 10-MeV protons. No single energy

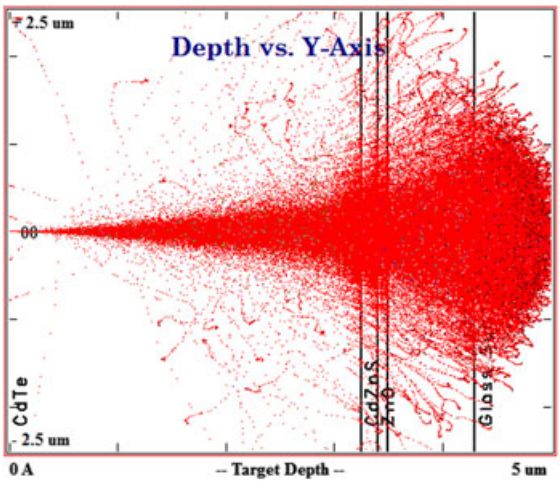

FIGURE 3 0.5-MeV proton longitudinal penetration in the CdTe solar cell deposited on the cerium doped cover glass [Colour figure can be viewed at wileyonlinelibrary.com]

radiation test can draw this equivalence directly; however, estimates can be made. The non-ionising energy loss (NIEL) for 0.5-MeV protons in CdTe is ~5000 times that for 1-MeV electrons, and given a typical 1 MeV electron fluence of ~10^{15} cm^{-2} for a 7-year geostationary Earth orbit (GEO) mission, it can be concluded that the lowest 0.5 MeV proton fluence of 1 × 10^{12} cm^{-2} would be representative of the damage incurred in a GEO mission lifetime of ~20 years.

The sample shown in Figure 2 was subject to the highest proton fluence of 1 × 10^{15} cm^{-2}. The darkened circle in the Perspex signifies the area of the proton beam. No visible changes to the 9 cells or the surrounding CdTe material were observed for all irradiated samples. Finally, an un-irradiated control sample was subject to the same storage conditions and then characterised alongside the proton irradiated samples. For comparison, a simulation was made for 10-MeV protons. These would pass through the entire structure (semiconductors and cover glass), causing much less damage and displacement (~0.6 per proton, ~24 eV per recoil).

2.3 | Solar cell characterisation

The AM1.5G solar cell performance was measured using an ABET Sun 2000 solar simulator calibrated with a GaAs reference cell supplied by L.O.T. oriel. Each sample was subject to a 10-minute light soak before measurement of the 9 cells. The device area was defined by 0.25-cm^2 evaporated gold contacts. All samples exhibited initial solar cell efficiencies in the range of 12.0 and 16.0%. External quantum efficiency (EQE) measurement of 3 of the 0.25 cm^2 cells per sample was made using a Bentham PV300 spectrometer, calibrated using a certified silicon photodetector.

Capacitance versus voltage measurements were conducted on 3 of the 0.25 cm^2 cells per sample using a Modulab XM ECS from Solartron Analytical. The samples were measured in the dark, at a fixed ambient temperature of 21° C. The DC voltage bias sweep was conducted between −3 and 2 V, with an applied 10-mV AC voltage at a fixed frequency (300 kHz) to measure the capacitance at the depletion edge for every sweep step of 0.05 V. The majority carrier

concentration depth profile can then be calculated based on the Mott-Schottky plots.

2.4 | Inert atmosphere anneal of irradiated solar cells

A post-proton irradiation anneal was carried out on Sample 3, which experienced a fluence of 1×10^{14} cm^{-2} and Sample 5, the control. Using a Carbolite™ tube furnace, under a nitrogen atmosphere and at atmospheric pressure, the samples were held at 100°C for 168 hours. This test closely simulates MIL-883—method 1019.8.

3 | RESULTS

Five CdTe on ultra-thin cover glass samples were prepared following the methodology described in Section 2.1. The samples were clamped into Perspex holders which serve 2 purposes: to facilitate electrical contact to the exposed TCO front contacts and to provide mechanical stability during characterisation and proton irradiation. The 5 samples were measured in the CSER laboratory for AM1.5G performance before being transported to the Surrey Ion Beam Centre for proton irradiation. Four of the samples were loaded onto a platen and subjected to the 4 different fluences of 0.5-MeV energy protons. The fifth sample was not irradiated and served as a control. The 0.5-MeV protons were shown by simulation to penetrate the PV structure such that they cause peak ionisation in the AZO layer just before the glass substrate interface. Table 1 provides a summary of the J-V performance for each of the samples, pre, and post proton fluence irradiation.

Table 1 shows that the lateral resistance of the TCO, the B2B resistance, remains unchanged, within experimental error, after proton irradiation. Small sample to sample difference arises due to variations in the underlying TCO conductivity, thickness of the high resistivity ZnO layer, and resistance between the TCO and copper tape contacts. The stability of the B2B to such high levels of proton fluence confirms that any change in device performance is not attributable to TCO performance. Table 1 also shows the before and after average cell performance of the PV cells.

Figure 4A shows the mean relative efficiency (Eff) of the 4 samples versus their respective proton fluence. For the lowest fluence of 1×10^{12} cm^{-2}, the mean solar cell efficiency decreased by 5%. Figure 4A shows that, for the CSER deposited CdTe and moving to a fluence of 1×10^{13} cm^{-2}, the mean efficiency drops by 18%, which is again above the 80% of B.O.L. performance that is required for a solar

TABLE 1 Mean J/V parameters for 9 × 0.25 cm cells on each of the 5 samples before and after proton irradiation. Sample 4, subject to the highest proton fluence, did not produce a J-V curve after irradiation. The standard deviation (SD) for each average parameter did not show any significant change before and after irradiation. All SDs were in the range of Eff 0.3-1.4%, J_{sc} 0.5-1.5 mA/cm^2, V_{oc} 7-17 mV, and FF 1.1-4.5%. The B2B value is the bus bar-to-bus bar resistance (the lateral resistance of the TCO)

	Sample 1		Sample 2		Sample 3		Sample 4		Sample 5	
	1×10^{12} cm^{-2}		1×10^{13} cm^{-2}		1×10^{14} cm^{-2}		1×10^{15} cm^{-2}		None	
Fluence	Pre	Post	Pre	Post	Pre	Post	Pre	Post	Pre	Post
Eff. (%)	15.5	14.6	12.9	11.0	13.2	1.0	13.0	-	12.8	12.8
V_{oc} (mV)	786	764	792	716	794	515	769	-	802	800
J_{sc} (mA/cm^2)	25.1	25.4	21.5	24.2	22.0	2.8	22.7	-	21.1	21.3
FF (%)	78.8	75.2	75.9	63.5	75.2	69.3	74.7	-	75.4	75.0
B2B (Ω)	7	8	4	4	5	5	7	7	9	8

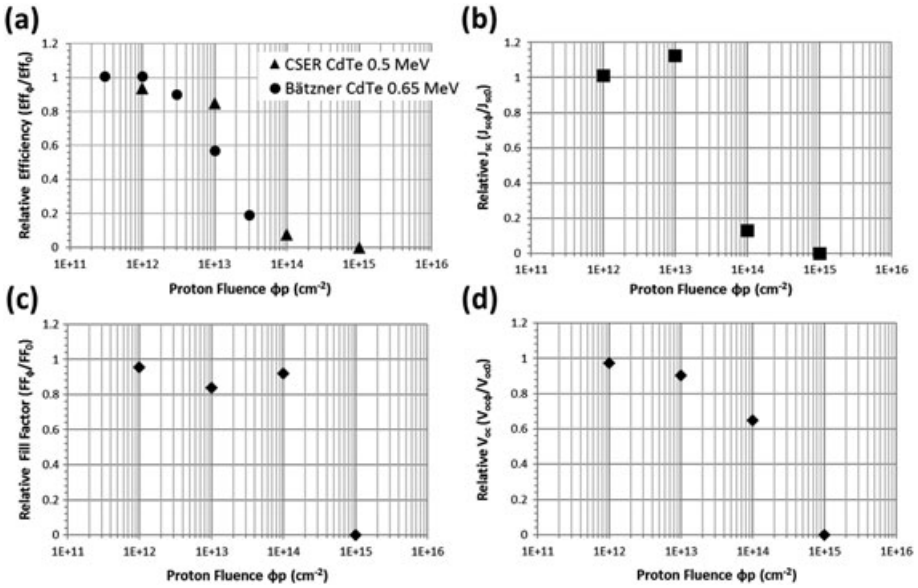

FIGURE 4 Mean J-V parameters of each of the samples (9 × 0.25 cm^2 cells per sample) after proton irradiation, expressed as a ratio to un-irradiated values, versus proton fluence (cm^{-2}). (A) Mean efficiency; (B) mean $J_{sc.}$; (C) mean V_{oc}; (D) mean FF

cell mission. It is between fluences of 1×10^{13} cm^{-2} and 1×10^{14} cm^{-2} where the devices reach their threshold of proton radiation tolerance. The relative mean efficiency drops by 96% when subject to a fluence of 1×10^{14} cm^{-2} and exhibits no photoresponse at fluence of 1×10^{15} cm^{-2}. The large drop in efficiency at 1×10^{14} cm^{-2} can be attributed to a large decrease in J_{sc}, shown in Figure 4B. The FF, shown in Figure 4C, has not shown a large decrease for this proton dose and a smaller decrease for V_{oc} than J_{sc} as can be seen in Figure 4D.

Bätzner et al used proton energies of 0.65 to 2.2 MeV and fluences of 1×10^{11} cm^{-2} and 1×10^{14} cm^{-2} directly incident on the cell layers.[8] As in this work, the lowest energy of 0.65 MeV was determined to be the most damaging for their cell structure. Figure 4A shows a comparison of the efficiency degradation with proton fluence obtained in this paper with the Bätzner et al 0.65-MeV data. At a fluence of 1×10^{13} cm^{-2}, the CdTe cells deposited onto the cover glass by MOCVD appear to show a significant improved proton degradation hardness that can be attributed to maintaining the transmission of the cerium doped cover glass at this proton dose. Unlike previous studies, which did not employ space quality cover glass, this decrease cannot be attributed to any darkening and therefore loss of optical transmission of the glass superstrate. This is perhaps the most interesting result from the proton irradiation measurements offering insight into the degradation pathway, without the complication of optical loss in the glass superstrate.

The large decrease in J_{sc} shown in Figure 4B was further investigated with EQE measurements of the cells. The EQE spectra taken from the cells following the different proton doses are shown in Figure 5. No significant change was observed in the EQE in Figure 5A, consistent with the measured J_{sc} for this cell. Some apparent increase is observed in Figure 5B following the 1×10^{13} cm^{-2} dose; most of this improvement is seen at longer wavelength, and the overall improvement is consistent with the apparent increase in J_{sc}. Figure 5C shows the before and after irradiation EQE for 1 cell from Sample 3 and was similar to 2 other cells measured from Sample 3. This shows the reason for the large drop observed in J_{sc} where the EQE was suppressed across most of the

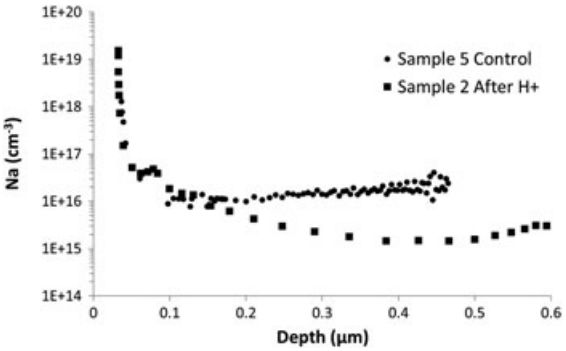

FIGURE 6 C-V depth profiles for un-irradiated sample 5 and sample 2 after 1×10^{13} cm^{-2} proton irradiation

spectrum with a spike in the EQE near the band edge of CdTe >775 nm. This EQE characteristic is consistent with conversion to n-type across some of the CdTe absorber layer thickness,[13] creating a buried junction.

Previous work has shown that, for the concentration of As doping detailed in Section 2.1, the MOCVD CdTe has a carrier concentration of around 5–10 × 10^{15} cm^{-3}.[14] Figure 6 confirms this carrier concentration in the control, Sample 5. When Sample 2 was subject to 1×10^{13} cm^{-2} proton fluence, the CdTe device carrier concentration was reduced by an order of magnitude from 1×10^{16} cm^{-3} to 1×10^{15} cm^{-3} but has retained most of the initial device efficiency, as can be seen in Table 1 and Figure 5B.

The evidence of the reduced carrier concentration for Sample 2 and the buried junction for the higher proton fluence, Sample 3, points to one of the following:

1. the As dopant concentration has been reduced
2. or compensated with shallow donors
3. or deeper trap defects moving the Fermi level away from the valence band edge.

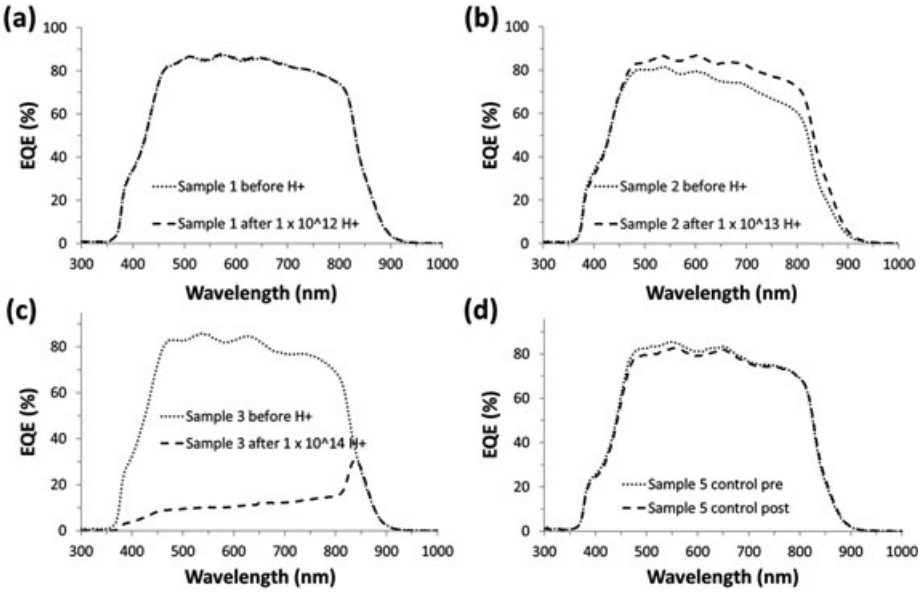

FIGURE 5 EQE spectra of pre and post proton irradiated samples. (A) Sample 1, 1×10^{12} cm^{-2}, (B) sample 2, 1×10^{13} cm^{-2}, (C) sample 3, 1×10^{14} cm^{-2}, (D) sample 5, the non-irradiated control

For Sample 3, with an EQE indicating a buried junction, the C-V measurements yielded a carrier concentration of 1×10^{14} cm^{-3}; 2 orders of magnitude below that of the control sample.

The proton energy was chosen to ensure absorption in the polycrystalline semiconductor layers, so it was effectively high energy hydrogen ion implantation. The role of high H^+ concentrations in the absorber layer as well as the effect of implantation damage requires further investigation. The buried junction characteristic of the EQE spectrum could be explained by the predicted absorption profile of the 0.5-MeV protons with a maximum absorption at the CdTe/CdZnS interface, pushing the junction back towards the more highly doped back contact layer (see Figure 3).

Figure 4D shows that the relative mean open circuit voltage only shows a rapid decrease for the highest proton dose. It would be expected that as the proton damage in the CdTe absorber layer, and at the junction, increases, then there would be a decrease in minority carrier lifetime and hence V_{oc} will decrease. An alternative explanation for the V_{oc} decrease would be a decrease in the acceptor concentration, which was observed. The complexing of proton implanted hydrogen, passivating the As dopant, could also create deep level centres that would reduce minority carrier lifetime and must be considered a possibility. However, this is not consistent with the FF in Figure 4C, which maintains its un-irradiated value up to the proton fluence of 1×10^{14} cm^{-2}.

The degradation mechanism was investigated further using an annealing treatment. Both Sample 3, after a proton fluence of 1×10^{14} cm^{-2}, and Sample 5, the control, were subject to an inert atmosphere anneal at 100°C for 168 hours as described in the experimental section. Figure 7 shows how this simple and a relatively low temperature anneal had a dramatic effect on recovering the EQE of the heavily irradiated Sample 3. No significant change was observed in the control PV cell. The Sample 3 efficiency was increased from 4% to 73% of its original performance. The relative mean J_{sc} of Sample 3, which had taken the most significant deterioration from the proton irradiation, was increased to above the initial mean J_{sc}, from 22.0 to 23.0 mA/cm^2. Figure 7 shows that this is due to an increase in the long wavelength EQE which is similar to the post irradiated EQE for the 1×10^{13} cm^{-2} proton dose of Sample 2.

The annealing mechanism of proton radiation damage can be expected to occur in space where solar arrays typically experience these annealing conditions (inert atmosphere and exposure to temperatures ≥100°C). The doses of protons that the samples have been subject to in this study would take many years to accumulate in the space environment; hence, this annealing and recovery mechanism could be expected to offset a significant amount of the damage observed in the solar cell performance at these proton fluences.

4 | DISCUSSION AND SOLAR CELL CAPACITANCE SIMULATOR (SCAPS) MODELLING

The degradation mechanism for the CdTe solar cells under intense proton irradiation was investigated using a SCAPS[15,16] model of the solar cells. The approach was to use established literature and measured parameters for the films in the PV structure as far as possible to minimize too many variable parameters to obtain a fit. The basic structure used for the model is as shown in Figure 1, but with the difference that for the SCAPS model, the CdTe absorber is divided into 3, with a near junction CdTe:S layer (reduced bandgap of 1.39 eV, 0.15 μm thick, to account for S interdiffusion,[17] acceptor concentration [$N_a = 1 \times 10^{16}$ cm^{-3}], the bulk of the absorber layer with a bandgap of 1.45 eV [3 μm thick, $N_a = 1 \times 10^{16}$ cm^{-3}], and a 0.2-μm back contact layer with $N_a = 1 \times 10^{18}$ cm^{-3}). N_a was independently measured by C-V profiling, for the un-irradiated cells, shown in Figure 6 to be 1×10^{16} cm^{-3}, which was used as the starting model value. The un-irradiated sample was used to establish the baseline parameters. The fitted parameters are shown in Table 2 and EQE in Figure 8, where the experimental and fitted EQE data can be compared. To fit the short wavelength edge, the $Cd_{1-x}Zn_xS$ bandgap and thickness were chosen to be 2.7 eV and 0.16 μm, respectively. It was also necessary to introduce a mid-gap neutral trap with a density of $N_t = 1.5 \times 10^{15}$ cm^{-3} which is consistent with work by Proskuryakov et al[18] on admittance

TABLE 2 Comparison of the J-V parameters for sample 1, prior to proton irradiation, with the SCAPS model parameters

	AM1.5G Eff. (%)	V_{oc} (mV)	J_{sc} (mA/cm^2)	FF (%)
Data	15.5	786	25.1	78.8
SCAPS	13.7	779	23.6	74.4

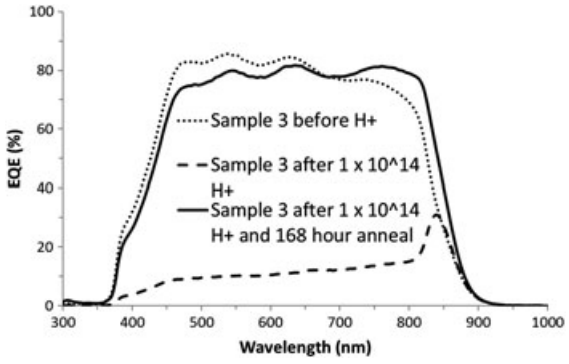

FIGURE 7 EQE before and after a proton irradiation dose of 1×10^{14} cm^{-2} for sample 3. The solid line shows the recovery of photoresponse after a 168-h anneal in nitrogen

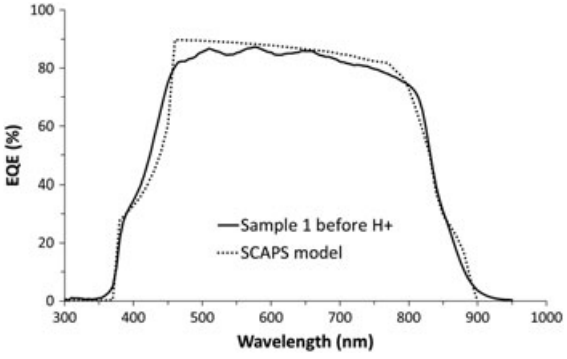

FIGURE 8 Comparison of the EQE for sample 1 before irradiation and the fitted SCAPS model

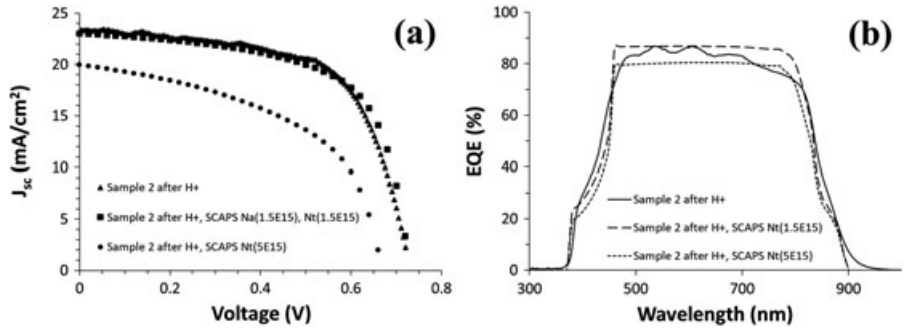

FIGURE 9 (A) Comparison of J/V for sample 2 following 1×10^{13} cm^{-2} proton irradiation and the SCAPS model with both N_a 1.5×10^{15} cm^{-3} and N_t 1.5×10^{15} cm^{-3} and N_a 1.5×10^{15} cm^{-3} and N_t 5×10^{15} cm^{-3}. (B) Comparison of EQE for sample 2 following 1×10^{13} cm^{-2} proton irradiation and the SCAPS model with both N_a 1.5×10^{15} cm^{-3} with N_t 1.5×10^{15} cm^{-3} and N_a 1.5×10^{15} cm^{-3} with N_t 5×10^{15} cm^{-3}

spectroscopy for As-doped CdTe solar cells. There were no other variable parameters to achieve this fit.

The approach taken with the irradiated solar cells was to keep these baseline parameters the same, as far as possible, and observe if the changes in EQE and J-V parameters could be reproduced through changing the absorber layer N_a and N_t. It was found, using the Sample 2, 1×10^{13} cm^{-2} data that a good fit could be obtained by reducing N_a to 1.5×10^{15} cm^{-3} (using the independently measured N_a from the C-V profile in Figure 6) and keeping N_t the same (for both CdTe:S and CdTe absorber layers), contrary to the expectation that proton damage would lead to an increase in N_t. The J-V and EQE curve fits are shown in Figure 9A,B and the J-V fit parameters in Table 3.

It can be seen from Figure 9A and Table 3 that this reduction in N_a without changing the value of N_t has enabled an excellent fit to the J-V data, increasing N_t to 5×10^{15} cm^{-3} resulted in poorer fits for both the J-V and the EQE data. One feature observed with the change in the EQE in Figure 5B is the improvement in EQE at longer wavelengths compared with the pre-irradiated solar cell. This can now be explained in terms of the larger depletion width with the much-reduced acceptor concentration, increasing from 0.2 to 0.8 μm. The reduction in the slope towards longer wavelength (500 to 800 nm) is clear in both the data and the SCAPS model and was noted both in Section 3 and Figure 4B when comparing with the un-irradiated sample. The main cause of the decrease in efficiency was attributed to the reduction in the V_{oc} and FF; both parameters were closely matched by the SCAPS model in Table 3 and did not require an increase in trap density as discussed as a possibility in Section 3. As the only change in the model parameters was the acceptor concentration in the CdTe:S and CdTe absorber layers, the observed reduction in efficiency of this proton irradiated cell can be clearly attributed to the reduction in N_a that was confirmed by C-V measurement.

For the recovery of the EQE and J-V parameters, following the low temperature anneal, the same model parameters were used as for the un-irradiated and 1×10^{13} cm^{-2} irradiated cells. The EQE fit, shown in Figure 10 and J-V parameters, shown in Table 4 are for $N_a = 8 \times 10^{14}$ cm^{-3}, $N_t = 1.5 \times 10^{15}$ cm^{-3} with no other change in model parameters from the baseline values. The C-V profile gave carrier concentration in the range 1×10^{14} to 1×10^{15} cm^{-3}. The SCAPS model clearly reproduces the flatter EQE from the blue to the near infrared region of the spectrum, and, as for the Sample 2 fit, this can be explained by a lower N_a increasing the depletion width and thus improving the collection at longer wavelengths.

The results of the SCAPS modelling of the proton irradiated solar cells shows that the deep trap concentration is not changing significantly, contrary to expectations, but the changes in device performance are due to changes in the acceptor concentration, verified by C-V measurement. Under the high dose of 1×10^{14} cm^{-2} protons, it is likely that the acceptors have been over-compensated with donors,

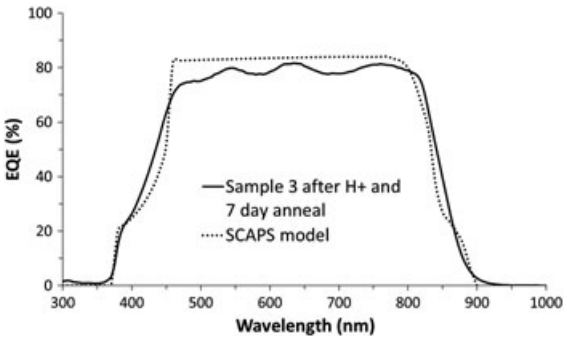

FIGURE 10 Comparison of EQE for sample 3 following 1×10^{14} cm^{-2} proton irradiation, followed by a 7-d low temperature anneal, and the SCAPS model with $N_a = 8 \times 10^{14}$ cm^{-3}

TABLE 3 Comparison of J/V parameters for sample 2 following 1×10^{13} cm^{-2} proton irradiation with the SCAPS model for $N_a = 1.5 \times 10^{15}$ cm^{-3} (from C-V measurement) and fitted $N_t = 1.5 \times 10^{15}$ cm^{-3}

	AM1.5G Eff. (%)	V_{oc} (mV)	J_{sc} (mA/cm^2)	FF (%)
Data	10.9	733	23.4	63.6
SCAPS	10.7	731	23.0	63.4

TABLE 4 Comparison of J/V parameters for sample 3 following 1×10^{14} cm^{-2} proton irradiation, and 7-d low temperature anneal, with the SCAPS model for $N_a = 8 \times 10^{14}$ cm^{-3}

	AM1.5G Eff. (%)	V_{oc} (mV)	J_{sc} (mA/cm^2)	FF (%)
Data	9.4	723	23.0	56.5
SCAPS	8.0	723	21.1	52.2

making the bulk of the absorber layer n-type. The partial recovery after a 7-day low temperature anneal indicated that the compensation was reversible. These results can be explained by the proton irradiation creating interstitial hydrogen forming a shallow donor. The proton irradiation dose is sufficiently high to create up to 5×10^{17} cm^{-3} donors if all the protons were absorbed in the CdTe layer, more than enough to compensate the active As acceptors. This is also consistent with the recovery following a low temperature anneal as hydrogen is a fast diffuser in CdTe.

5 | CONCLUSIONS

This study is the first to measure the effects of proton irradiation of CdTe solar cells deposited directly onto radiation hard cover glass. Using the cover glass as the superstrate has removed the darkening effects observed for non-cerium doped glass superstrates. Different proton energies at normal incidence on the CdTe side were simulated with SRIM simulations showing that 0.5-MeV protons would pass through all the active layers and also cause the maximum damage in terms of ionization energy deposited and displacement damage in the bulk of the CdTe absorber layer.

Four CdTe samples, each having 9 defined 0.25 cm^2 solar cells, were irradiated at 0.5 MeV and different doses of protons to represent different orbital environments and mission durations in space. At the lowest fluence 1×10^{12} cm^{-2}, the relative efficiency of the solar cells decreased by only 5%. This dose of protons could reasonably be expected to represent that experienced by a 20-year GEO mission. Once the proton dose was increased to 1×10^{13} cm^{-2} and then 1×10^{14} cm^{-2}, the solar cell relative efficiency decreased to 82% and 4%, respectively. This response to proton radiation was better than previous studies using CdTe and can be attributed to using cerium doped cover glass. Importantly, the efficiency following these doses is also more than 2 orders of magnitude better than conventional multi-junction devices. Device characterization by EQE of the irradiated cells showed that at the high dose of 1×10^{14} cm^{-2}, a buried junction was forming with a spike in the EQE near the CdTe band edge (> 775 nm).

The effect of the high intensity proton doses on degradation of the CdTe solar cells can be explained using SCAPS modelling. An excellent fit was obtained for the 1×10^{13} cm^{-2} dose sample with a reduction in N_a and no change in trap density, which was surprising but supported with C-V measurement.

A low energy thermal anneal (100°C), in a nitrogen atmosphere, was carried out on the sample that received the 1×10^{14} cm^{-2} dose. The anneal had the effect of restoring the solar cell efficiency to 73% of its pre-irradiated value. The SCAPS modelling provided a good fit to the recovered EQE and J-V parameters with removal of the buried junction and N_a restored to 8×10^{14} cm^{-3}. This indicated that the compensation was readily reversible and is consistent with the proton irradiation creating interstitial hydrogen, resulting in a shallow donor level. This study of 0.5-MeV proton irradiation for CdTe solar cells on a cerium doped cover glass over a wide range of fluences demonstrates a radiation hardness (to protons) that is far superior to conventional multi-junction III-V solar cells used for space. Further investigations will look at the effects of electron irradiation on the degradation mechanism of CdTe solar cells on the cover glass. This will be an opportunity to isolate radiation damage from the proton implantation mechanism.

ACKNOWLEDGEMENTS

The authors acknowledge financial support from the Engineering and Physical Science Research Council (EPSRC, Grant Ref. EP/K019597/1 and EP/K019597/2). Qioptiq Space Technology is thanked for the supply of space qualified cerium-doped cover glass.

ORCID

Dan A. Lamb http://orcid.org/0000-0002-4762-4641

REFERENCES

1. Lamb DA, Irvine SJC, Clayton AJ, et al. Characterization of MOCVD thin-film CdTe photovoltaics on space-qualified cover glass. *IEEE Journal of Photovoltaics*. 6(2):557-561.
2. Lamb DA, Irvine SJC, Clayton AJ, et al. Lightweight and low cost thin film photovoltaics for large area extra-terrestrial applications. *Renewable Power Generation, IET*. 2015;9(5):420-423.
3. Irvine SJC, Lamb DA, Clayton AJ, Kartopu G, Barrioz V. Cadmium telluride solar cells on ultrathin glass for space applications. *Journal of Electronic Materials*. 2014;43:2818-2823.
4. Kimber R, Lamb DA, Irvine SJC, Baker MA, Grilli R, Underwood CI, Hall J, Cadmium telluride thin film photovoltaics for space application, Proceedings of the 29th European Photovoltaic Solar Energy Conference, Amsterdam 2014: 2066–2071.
5. Herman DA, NASA's evolutionary xenon thruster (NEXT) project qualification propellant throughput milestone: performance, erosion, and thruster service life prediction after 450 kg, 57th Joint Army-Navy-NASA-Air Force (JANNAF) propulsion meeting, Colorado Springs, Colorado, USA, May 3–7, 2010.
6. Sebolt W. Space and earth based solar power for the growing energy needs of future generations. *Acta Astronaut*. 2004;55:389
7. Stroud JS. Photoionization of Ce^{3+} in glass. *J Chem Phys*. 1961;35 (3):844-850.
8. http://www.qioptiq.com/space.html
9. Bätzner DL, Romeo A, Terheggen M, Döbeli M, Zogg H, Tiwari AN. Stability aspects in CdTe/CdS solar cells. *Thin Solid Films*. 2004;451–452:536-543.
10. Romeo A, Bätzner DL, Zogg H, Tiwari AN. Influence of proton irradiation and development of flexible CdTe solar cells on polyimide. *Mat Res Soc Symp Proc*. 2001;668:H3.3.1-H3.3.6.
11. Yang G, Cho EW, Wang YJ, et al. Radiation hard and ultra-lightweight polycrystalline CdTe thin film solar cells for space applications. *Energ Technol*. 2016; https://doi.org/10.1002/ente.201600346
12. Ziegler JF, Biersack JP, and. Ziegler MD, SRIM—the stopping and range of ions in matter, http://www.SRIM.org (2008). Accessed: February 5, 2017.
13. Gretener C, Wyss M, Perrenoudm J, Kranz L, Buecheler S, and Tiwari AN, CdTe thin films doped by Cu and Ag—a comparison in substrate configuration solar cells, 2014 IEEE 40th Photovoltaic Specialist Conference: 3510–3514.
14. Kartopu G, Phillips LJ, Barrioz V, et al. Progression of metalorganic chemical vapour-deposited CdTe thin-film PV devices towards modules. *Progress in Photovoltaics: Research and Applications*. 2016;24:283-291.
15. Burgelman M, Nollet P, Degrave S. Modelling polycrystalline semiconductor solar cells. *Thin Solid Films*. 2000;361-362:527-532.
16. Burgelman M and Marlein J, Analysis of graded band gap solar cells with SCAPS, Proceedings of the 23rd European Photovoltaic Solar Energy Conference, (Valencia, E, September 2008): 2151–2155.

17. Taylor AA, Major JD, Kartopu G, et al. A comparative study of microstructural stability and sulfur diffusion in CdS/CdTe photovoltaic devices. *SOLMAT*. October 2015;141:341-349.
18. Proskuryakov YY, Durose K, Major JD, et al. Doping levels, trap density of states and the performance of co-doped CdTe (As,Cl) photovoltaic devices. *Solar Energy Materials and Solar Cells*. 2009;93:1572-1581.

How to cite this article: Lamb DA, Underwood CI, Barrioz V, et al. Proton irradiation of CdTe thin film photovoltaics deposited on cerium-doped space glass. *Prog Photovolt Res Appl*. 2017; 1–9. https://doi.org/10.1002/pip.2923